

Supplement

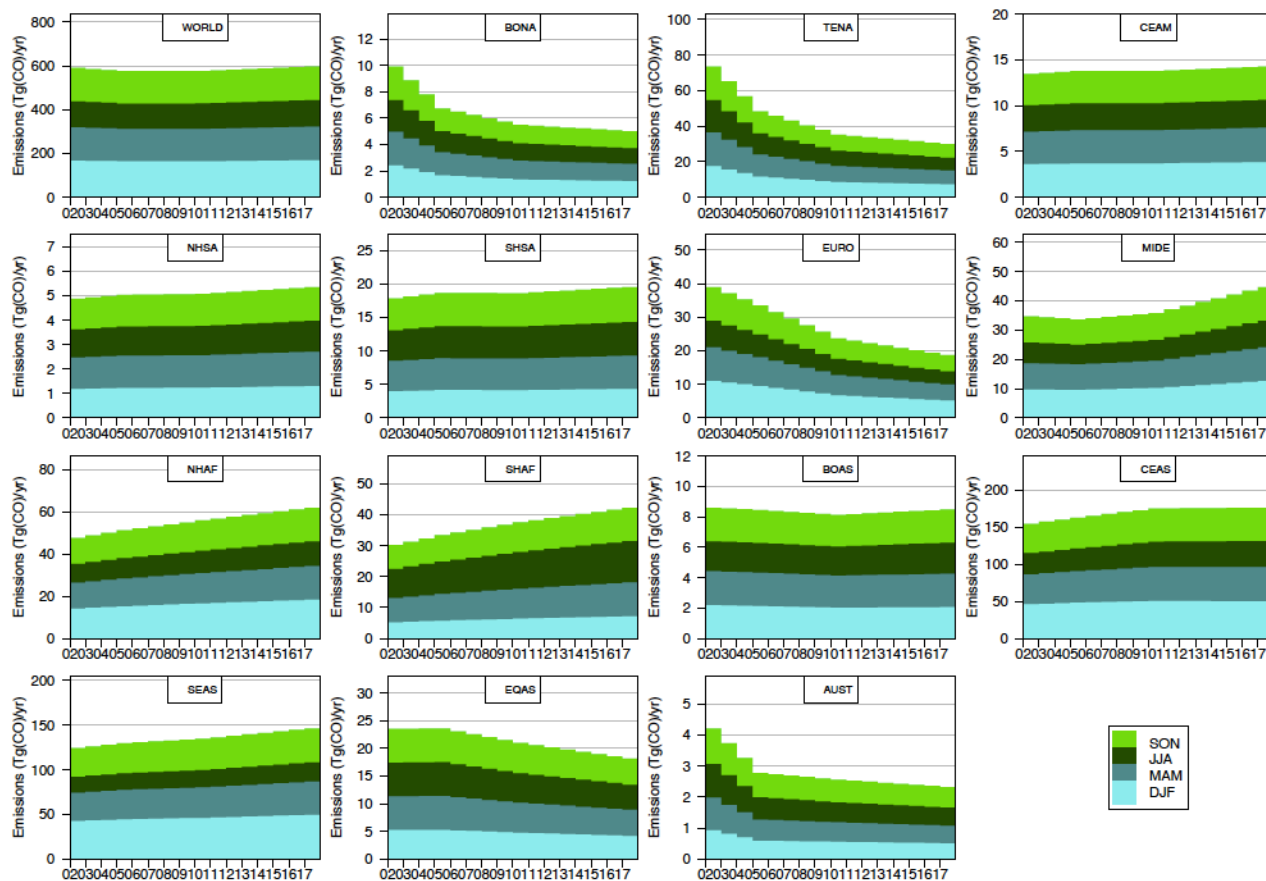
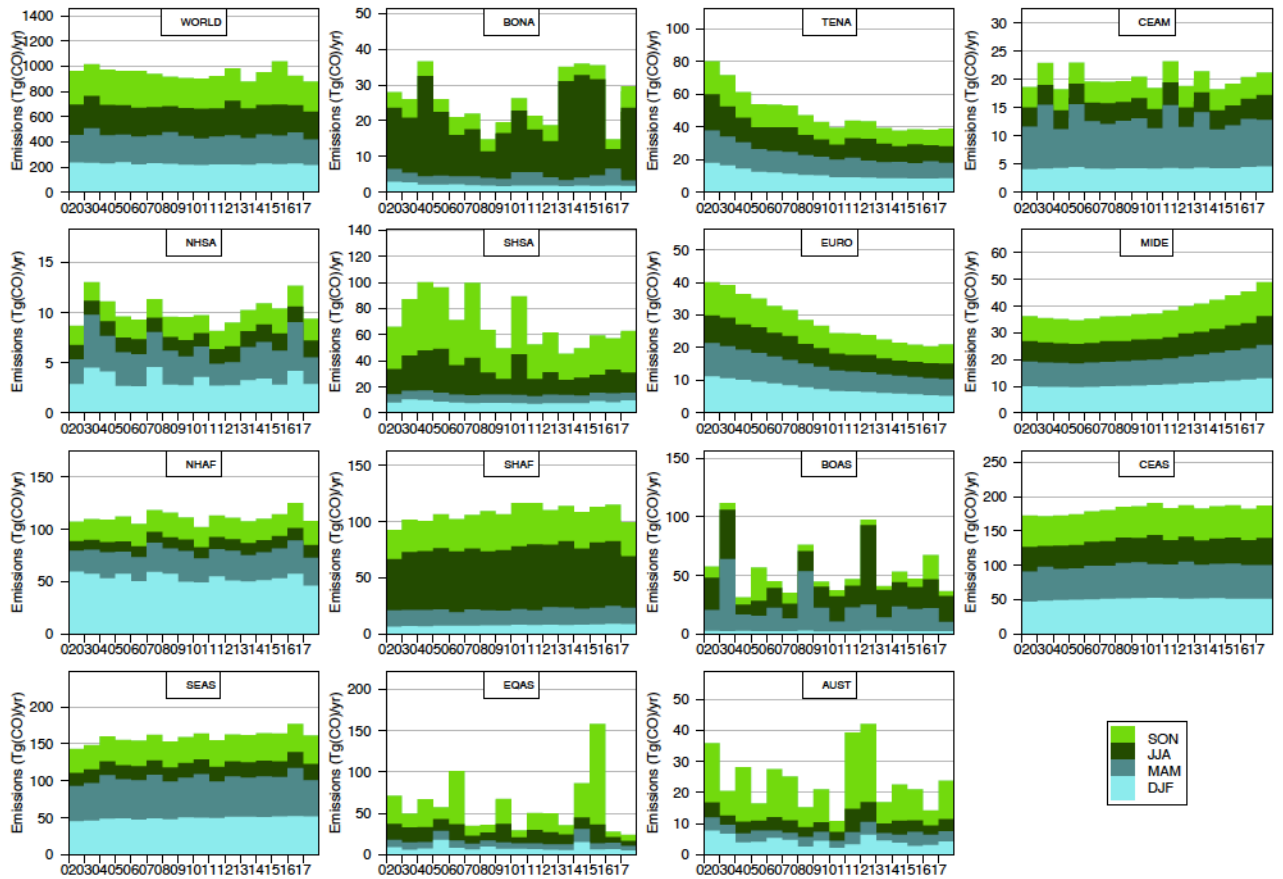
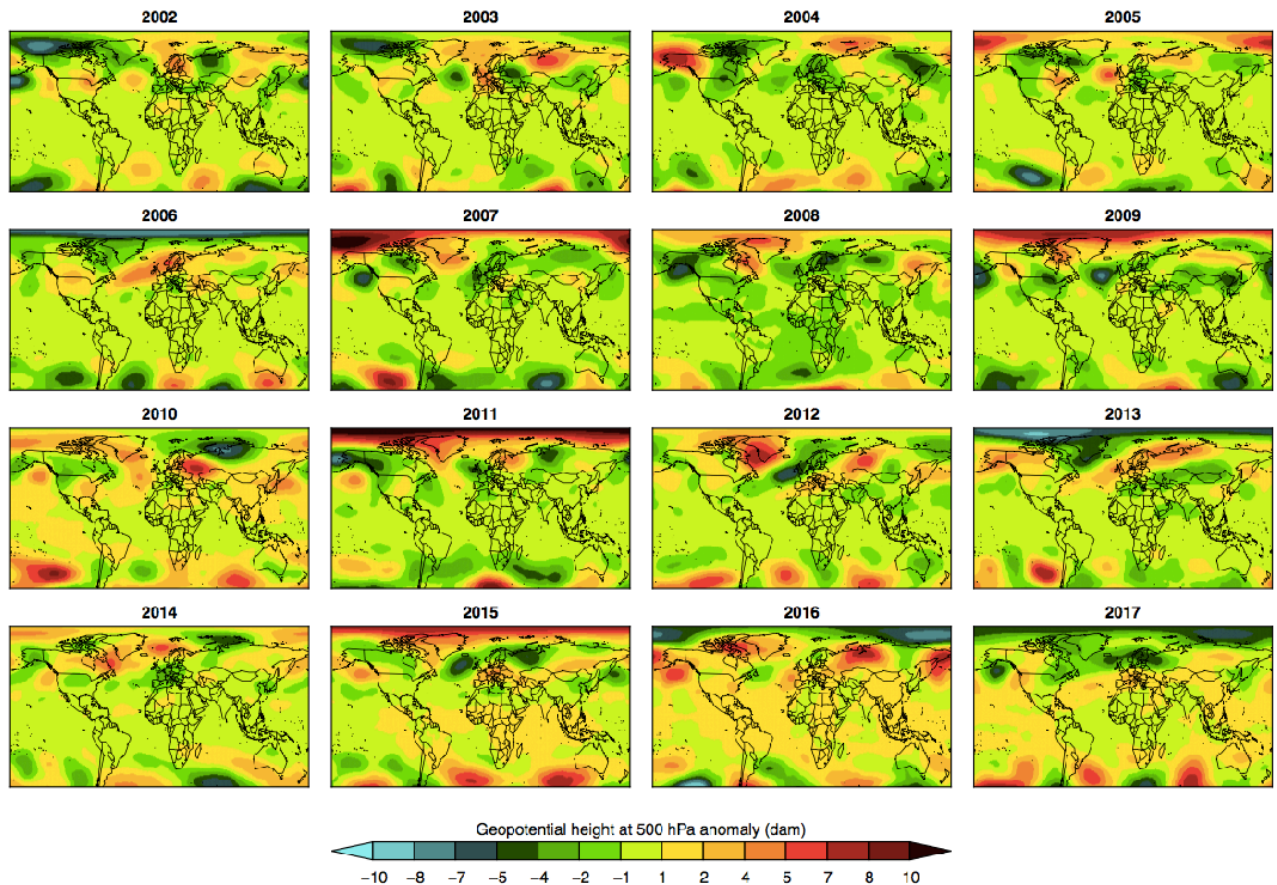


Figure S1: Cumulated seasonal MACCity anthropogenic CO emissions at the global scale and in the 14 continental regions. Seasons are winter (DJF), spring (MAM), summer (JJA) and autumn (SON).



**Figure S2: Cumulated seasonal total (anthropogenic and biomass burning) CO emissions at the global scale and in the 14 continental regions.** Seasons are winter (DJF), spring (MAM), summer (JJA) and autumn (SON). Biomass burning emissions are from GFASv1.0 in 2002 and from GFASv1.2. over the 2003-2017 period, anthropogenic emissions are from MACCity.



**Figure S3: Annual seasonally-averaged geopotential height (Z500) anomalies during summer (June-August) regarding the 1974-2014 climatology.** Data come from the ERA-interim reanalysis. Several situations of anticyclonic conditions (positive Z500 anomalies) appear associated with severe fire episodes, e.g. eastern Siberia in 2003, north-western Canada (Yukkon territory; 1,720,324 ha burned) in 2004, western Russia in 2010, south-eastern Canada (Quebec; 1,872,842 ha burned) in 2013.

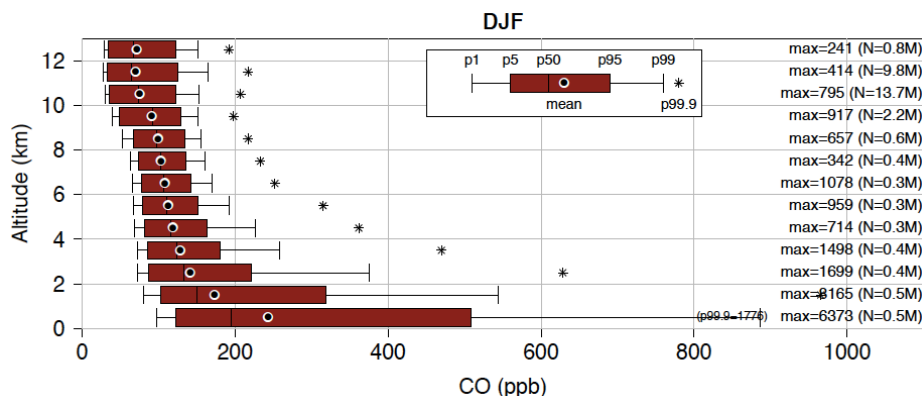


**Figure S4: Distribution of the CO mixing ratios measured by MOZAIC-IAGOS aircraft during the 2002-2017 period in winter (DJF).** Results are shown per 1 km-width layer, without any discrimination between troposphere and stratosphere (N gives the number of points in millions, pX in the legend indicates the X<sup>th</sup> percentile of the distribution).

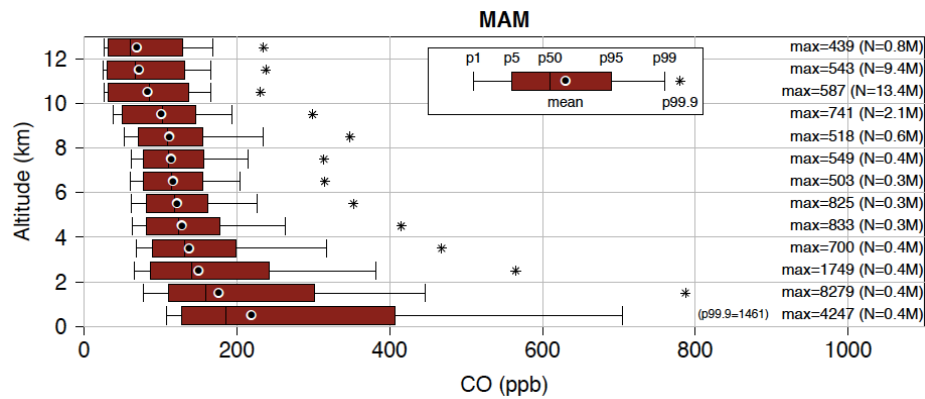


Figure S5: Same as Fig. S4 at spring (MAM).

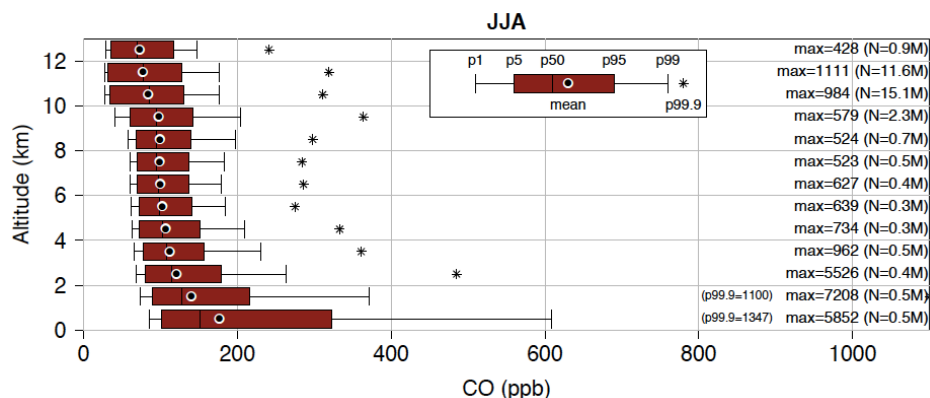


Figure S6: Same as Fig. S4 at summer (JJA).

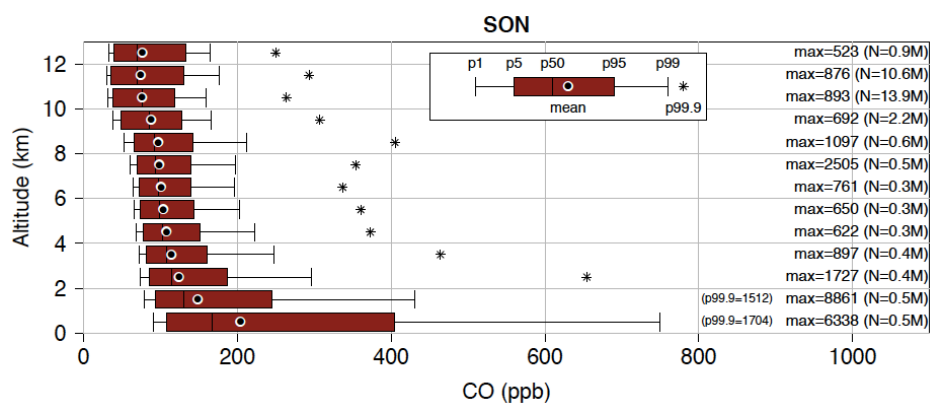
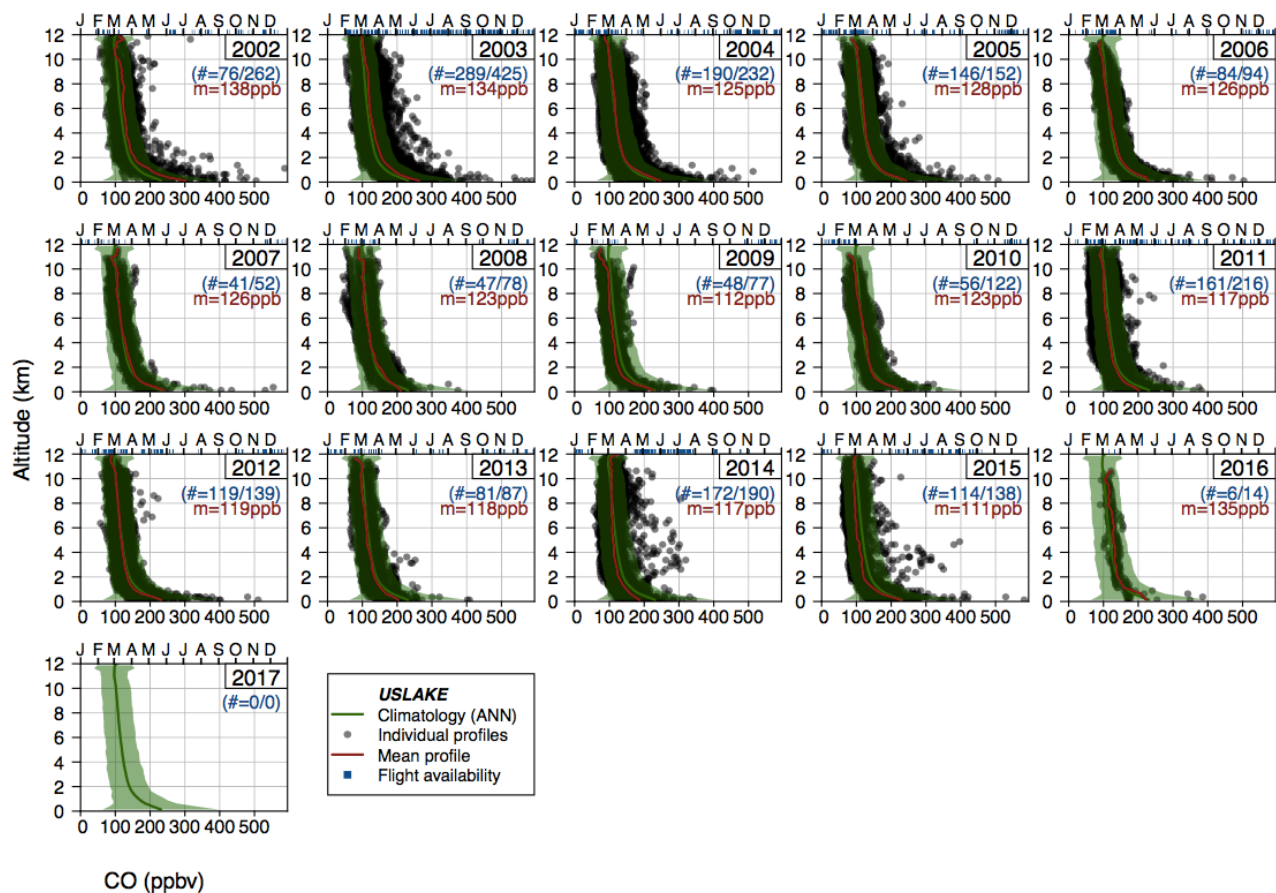


Figure S7: Same as Fig. S4 at fall (SON).



**Figure S8 : Overview of CO mixing ratio profiles at USLAK.** All individual CO profiles sampled between 2002 and 2017 are shown with black points (a transparency is added to better highlight the density of points), and the corresponding average profile in red. The mean climatological vertical profile over the period 2002-2017 is shown with a green line (the green area corresponds to  $\pm 2\sigma$ ). The plot also shows in blue the number of vertical profiles and their distribution along the year (a blue bar on the time axis above graphs indicates that a flight is available on that day; this time axis does not correspond to the abscissa of the plot).



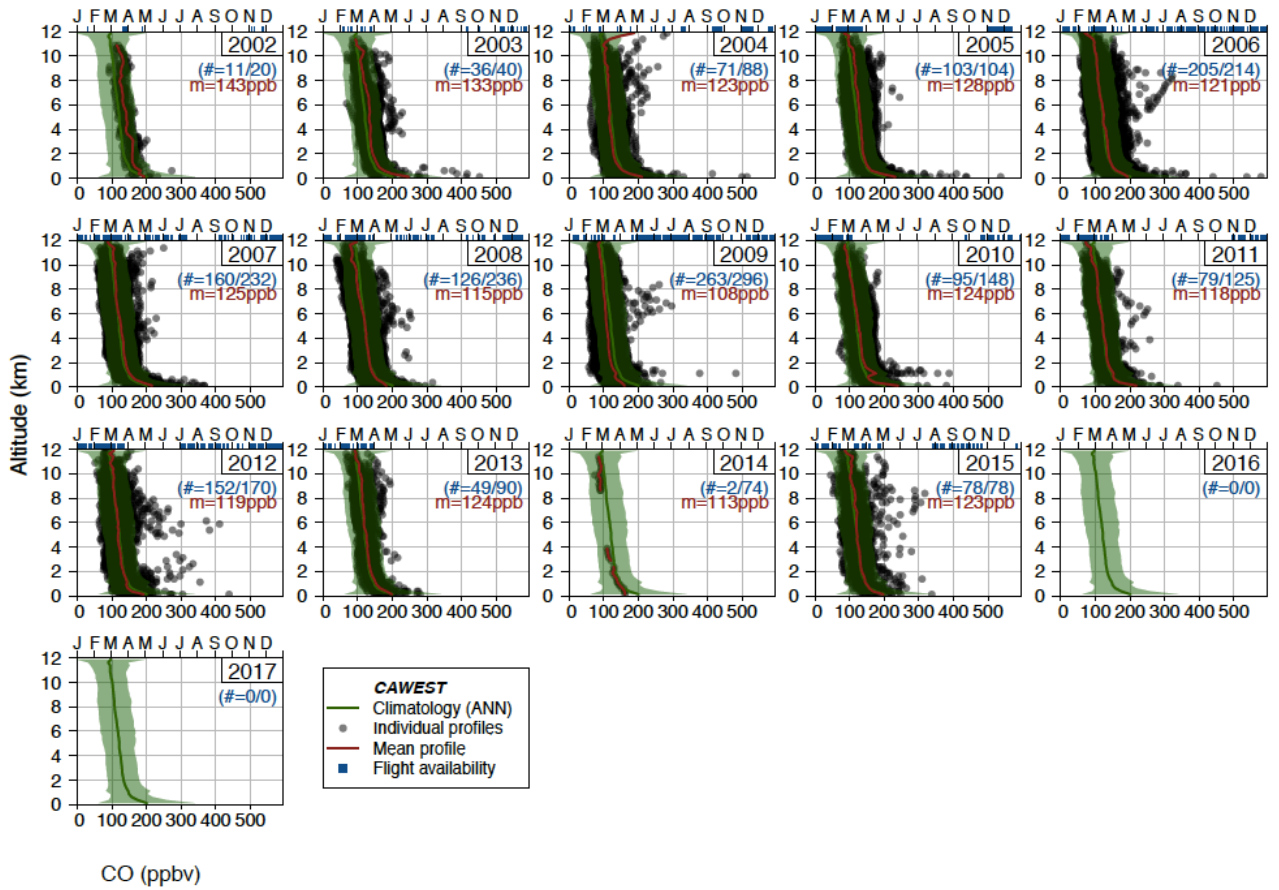


Figure S9: Same as Fig. S8 at CAwest cluster.

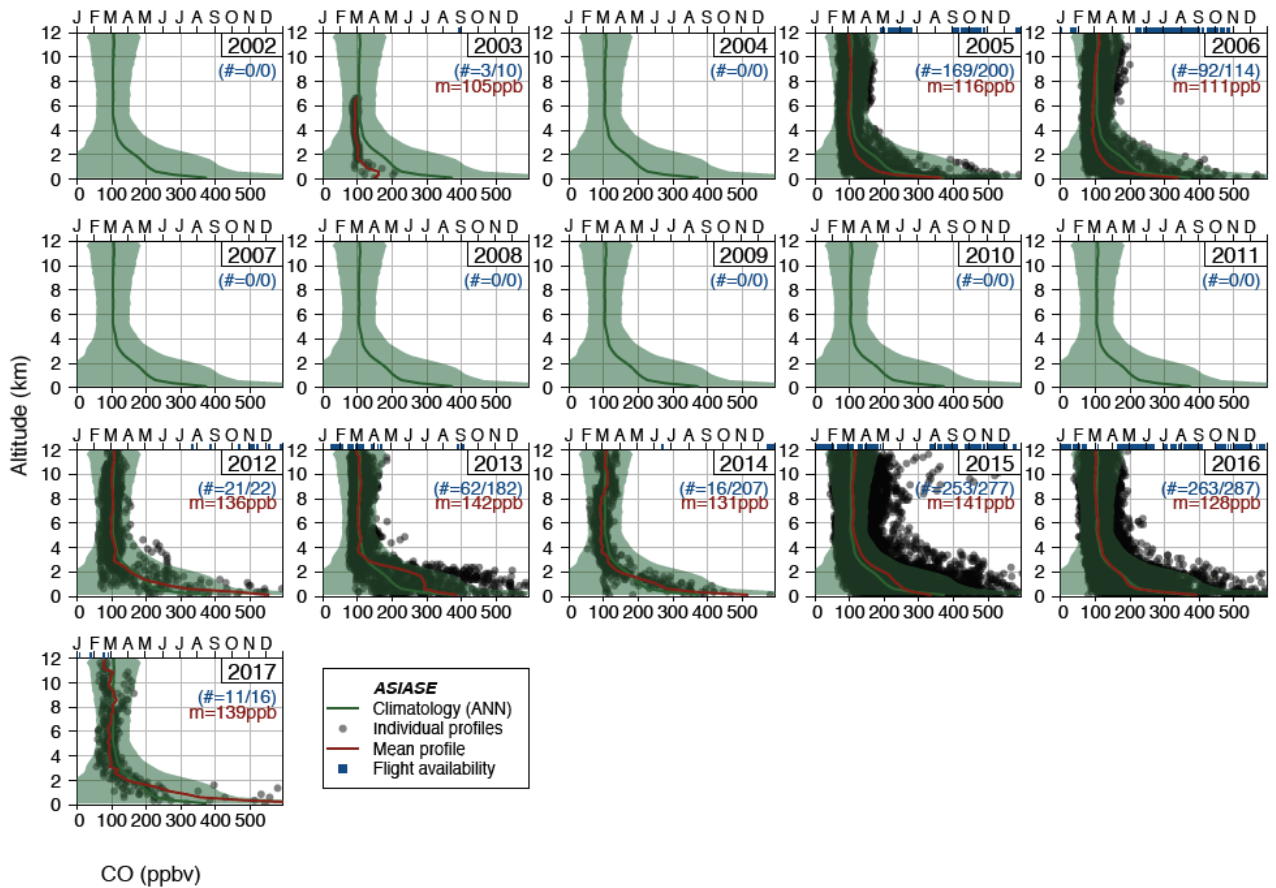
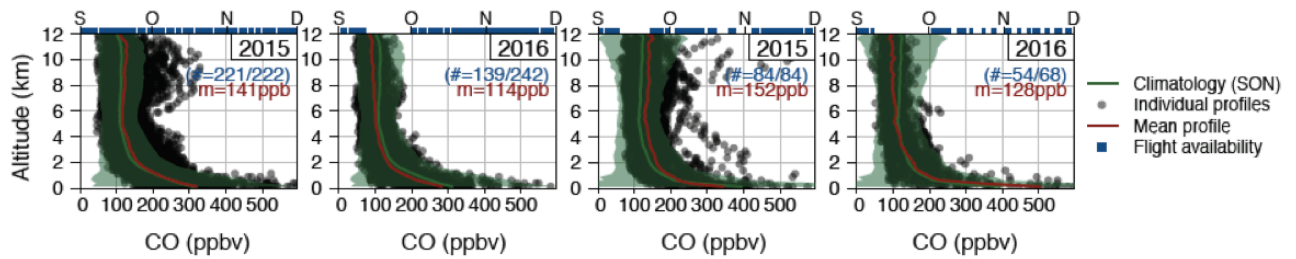
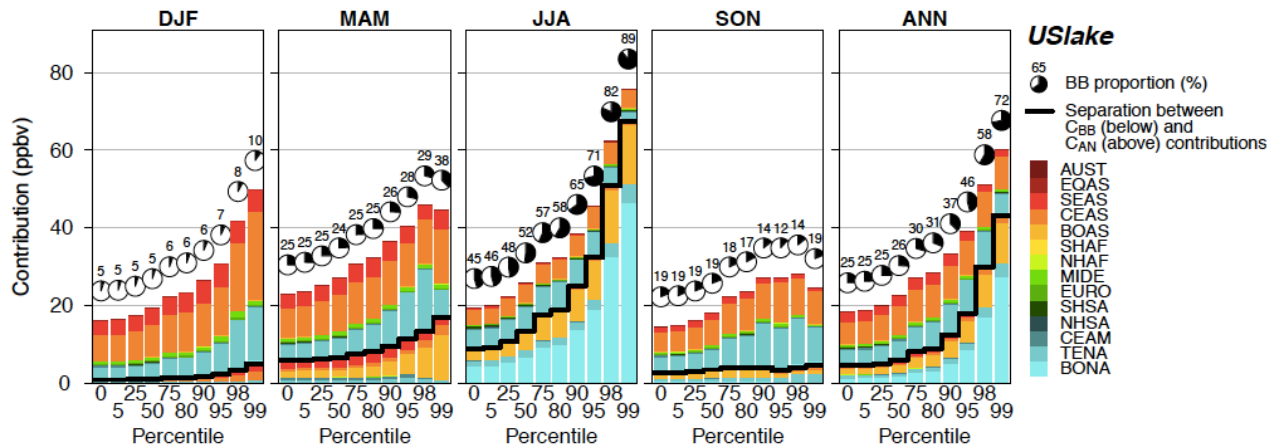


Figure S10: Same as Fig. S8 at AsiaSE cluster.



**Figure S11 : Overview of CO mixing ratio profiles during fall (SON) season in at ChinaSE (two left panels) and AsiaSE (two right panels).** All individual CO profiles sampled in fall 2015 and 2016 are shown with black points (a transparency is added to better highlight the density of points), and the corresponding average profile in red. The mean seasonally-averaged vertical profile over the period 2002-2017 is shown with a green line (the green area corresponds to  $\pm 2\sigma$ ). The plot also shows in blue the number of vertical profiles and their distribution along the season (a blue bar on the time axis above graphs indicates that a flight is available on that day; this time axis does not correspond to the abscissa of the plot).



**Figure S12 : Mean AN and BB contributions at the USlake airport cluster.** Results are shown for all seasons and different anomalies subsets (designated by the corresponding percentile). The geographic origin of both types of CO emissions is indicated by the colours. The dark line separates the BB (below) and ANN (above) contributions. The relative contribution of BB is reported with a pie.

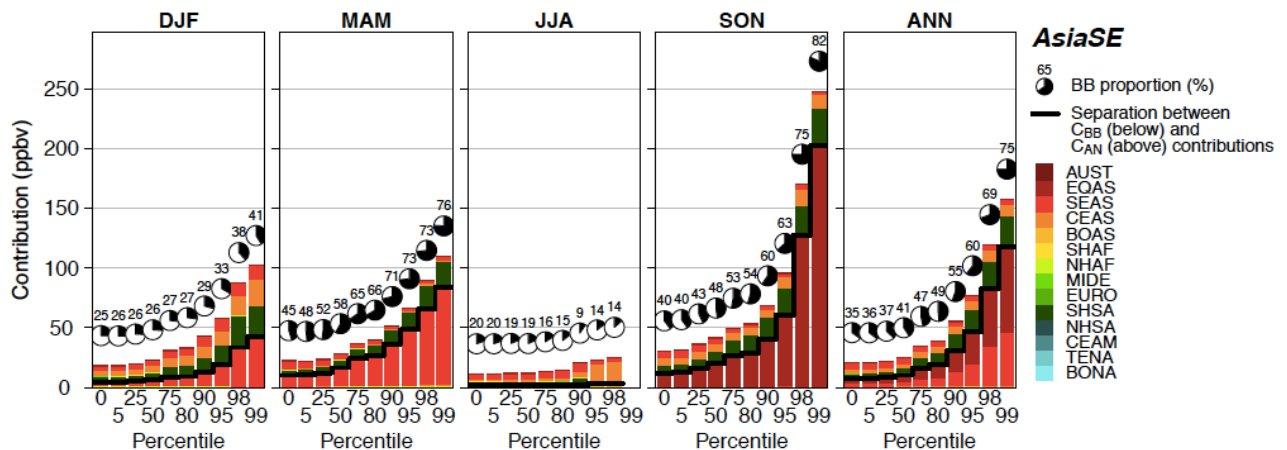


**Figure S13 : Same as Fig. S12 for AsiaSE cluster.**